

# Through-thickness analysis of the skin layer thickness of multi-layered biaxially-oriented polypropylene films by micro-thermal analysis

Guy Van Assche<sup>a,\*</sup>, Antoine Ghanem<sup>b</sup>, Olivier Lhost<sup>c</sup>, Bruno Van Mele<sup>a</sup>

<sup>a</sup>Physical Chemistry and Polymer Science, Vrije Universiteit Brussel, Pleinlaan 2, B-1050 Brussels, Belgium

<sup>b</sup>Solvay SA, Central Management Research and Technology, Analytical Technologies, rue de Ransbeek 310, B-1120 Brussels, Belgium

<sup>c</sup>BP Belgium NV, Polymers Europe RD&T, rue de Ransbeek 310, B-1120 Brussels, Belgium

Received 12 October 2004; accepted 29 April 2005

Available online 22 June 2005

## Abstract

A novel method is presented for the determination of the thickness of a polymer layer on a solid substrate by through-thickness local thermal analysis (LTA) measurements using a micro-thermal analyser ( $\mu$ TA). The feasibility of the method is illustrated for a poly(methyl methacrylate) film spin-cast on a silicon wafer. Subsequently the method is applied to determine the skin layer thickness of multi-layered biaxially-oriented polypropylene (BOPP) films. Although the melting temperatures of skin and core layer are only 15 °C different, it proved to be possible to determine the skin layer thickness. The film thickness obtained by  $\mu$ TA correlates well with the thickness observed by transmission electron microscopy (TEM) in a 0.1–1.6  $\mu$ m range. The method is shown to be accurate, robust, and fast.

© 2005 Elsevier Ltd. All rights reserved.

**Keywords:** Micro-thermal analysis; Biaxially-oriented polypropylene; Polymer films

## 1. Introduction

Biaxially oriented polypropylene (BOPP) films, both heat sealable and non-heat sealable are extensively used in the food and non-food packaging industry [1]. These films are uni- or multi-layered structures having a typical total thickness of only 15–25  $\mu$ m. The simplest multilayer films correspond to three-layer structures: one thick core layer of polypropylene homopolymer sandwiched between two thin (usually close to 1  $\mu$ m) skin layers. Other films exist on the market with 5, 7 or even 9 layers; as well as sophisticated structures obtained by laminating BOPP films with other layers.

Each layer has its own contribution to the properties of the film. In the standard three-layer structures, the core layer mainly provides the rigidity of the film, whereas the skin layers provide sealing and/or surface properties. Thus, it is intuitively evident that, even excluding any cost

consideration, the thickness of each layer is an important parameter for the film properties.

To determine the thickness of the 0.1–2  $\mu$ m thick skin layers is not an easy task. Transmission electron microscopy (TEM) and spectroscopic ellipsometry can be employed. However, a major disadvantage for TEM is the extensive sample treatment needed, involving embedding, cross-sectioning, and (often) etching of the films. For quantitative layer thickness measurements, care needs to be taken that the layered structure is not influenced by the thermal treatment, during embedding, and by the mechanical loads exercised with the ultra-microtome. For the biaxially-oriented co-extruded films studied here, a further complication is the chemical similarity of skin and core layer, which strongly limits the contrast on the one hand, and the options for inducing contrast by etching, on the other hand. This chemical similarity of skin and core layers also limits the difference in the index of refraction of the layers, rendering the use of spectroscopic ellipsometry more difficult. Additionally, the modelling of the layered structure needed for analysing the results is complicated by the absence of accurate optical properties for the constituent materials of the layers, possible surface roughness, crystallisation and orientation effects and, generally speaking, by

\* Corresponding author. Tel.: +32 2 6293276; fax: +32 2 6293278.  
E-mail address: [gvanassche@vub.ac.be](mailto:gvanassche@vub.ac.be) (G. Van Assche).

the presence of a rough, possibly diffuse interface, and interphase formation between the layers.

The above-mentioned complications related to embedding and microtomy procedures can be even more severe for a scanning probe microscopy (SPM) analysis of cross sections of the film. In this paper, we will show that these complications can be avoided by through-thickness analyses of the films using micro-thermal analysis ( $\mu$ TA). This technique combines an SPM with a Wollaston-type thermal probe, enabling imaging and local thermal analysis [2,3]. Barral and co-workers [4] characterised BOPP-films by atomic force microscopy (AFM) and micro-thermal analysis ( $\mu$ TA). From topographic AFM-images of the film surface, information is gained about the homogeneity of the surface of metallised films and in the presence of additives. By imaging embedded cross-sections, the total film thickness was determined (range 15–60  $\mu$ m). In local thermal analysis mode, the melting of the core layer could be measured. In the images, skin layers with a thickness of 1  $\mu$ m or less could not be detected due to the resolution of the thermal probes.

## 2. Experimental

### 2.1. Materials

Co-extruded, biaxially-oriented films with an isotactic polypropylene (iPP) core layer (about 20  $\mu$ m thick) and with a skin layer with a thickness between 0.1 and 1.6  $\mu$ m were studied. The skin layer material is a copolymer of propylene with  $\alpha$ -olefins. All films and raw materials were kindly supplied by Solvay SA and BP Belgium NV.

For thermal and rheological characterisations of the raw constituent materials, pellets of core and skin layer material were used. Films of 0.25 mm thickness were prepared in a High Temperature Constant Thickness Film Maker (Graseby Specac Ltd) by melting pellets between aluminium foils at 200  $^{\circ}$ C using 2 ton pressure for 5 min, and subsequently cooling the press to about 50  $^{\circ}$ C while maintaining the pressure.

Poly(methyl methacrylate) (PMMA) of molar masses of 15,000, 93,300, and 350,000  $\text{g mol}^{-1}$  (secondary standards) were obtained from Acros. PMMA (93,300  $\text{g mol}^{-1}$ ) was spin-coated onto a silicon wafer from a dichloromethane solution and subsequently dried under vacuum at 100  $^{\circ}$ C for 12 h and at 115  $^{\circ}$ C for 15 min. For all molecular weights, films of 0.25 mm thickness were prepared as described above for the core and skin layer materials, using a maximum temperature of 25  $^{\circ}$ C above the glass transition temperature.

### 2.2. Techniques

#### 2.2.1. Micro-thermal analysis

The TA Instruments 2990 Micro-Thermal Analyser

( $\mu$ TA) combines an atomic force microscope (AFM) with Wollaston-type thermal probes and a temperature-controlled stage. All measurements were performed in air.

Topography and conductivity images are obtained by scanning the probe over the surface while maintaining it at a constant temperature. Local thermal analyses (LTA) are performed by positioning the tip at a selected location and subsequently heating it, resulting in a sensor ( $\mu$ TMA) and a power signal ( $\mu$ DSC).

The calibration of the sensor signal (the vertical displacement of the probe during LTA) was verified using PMMA ( $M_w = 93,300 \text{ g mol}^{-1}$ ) films spin-coated onto  $8 \times 8 \text{ mm}^2$  silicon wafers from a methylene chloride solution. A thermolithographic procedure was developed for measuring the thickness of these films in a surface mapping with the micro-TA (see below).

Micro-thermal analyses of BOPP films were performed on  $4 \times 4 \text{ mm}^2$  of film, cut from a larger foil and fixed onto metallic sample stubs using double-sided sticky tape. Images of  $100 \times 100 \mu\text{m}^2$  (200 lines) were recorded at a scan speed of 100  $\mu\text{m/s}$  with the probe at 50  $^{\circ}$ C and using a contact force corresponding to 10 nA (1 nA corresponds to 3–4 nN). In each image, five locations were selected for analysis by LTA. The probe is heated from 0 to 225  $^{\circ}$ C at a heating rate of 5  $^{\circ}$ C/s using contact forces corresponding to 10 nA (except mentioned otherwise).

#### 2.2.2. Transmission electron microscopy

BOPP-film samples were embedded in an epoxy resin. After curing, sections of nominal 90 nm thickness were obtained by ultra-microtomy. These sections were examined with a Siemens Elmiskop 101 microscope at 60 keV accelerating voltage. The layer thickness was measured on  $10,000 \times$  magnification prints. A thickness above 0.1  $\mu$ m can be measured with estimated errors of  $\pm 0.06 \mu\text{m}$  at a thickness of 0.10  $\mu\text{m}$  and  $\pm 0.20 \mu\text{m}$  at a thickness of 1.5  $\mu\text{m}$ .

#### 2.2.3. Differential scanning calorimetry (DSC)

The melting of the bulk core and skin layer materials of the films were studied by DSC using a TA Instruments Q1000 differential scanning calorimeter equipped with a refrigerated cooling system. The instrument was calibrated for temperature and enthalpy using the melting of indium.

A sample of about 3 mg was placed in an aluminium crucible (TA Instrument). The samples were first heated to 180  $^{\circ}$ C at 10  $^{\circ}$ C/min and kept isothermally for 3 min. After cooling at 10  $^{\circ}$ C/min to  $-50 \text{ }^{\circ}$ C, the melting was studied in a subsequent heating at 10  $^{\circ}$ C/min to 180  $^{\circ}$ C.

#### 2.2.4. Dynamic rheometry (small angle oscillatory shear measurements)

The melt rheology of the raw materials was studied using a TA Instruments AR1000N controlled-stress rheometer equipped with an extended temperature module. The

measurements were made in small angle oscillatory shear mode using parallel plates.

A sample disc of 4 cm diameter and about 0.50 mm thickness was placed between two 4 cm disposable aluminium plates for measurement in a parallel plate set-up. The samples were heated to 220 °C for 15 min to remove thermal history effects and subsequently cooled to the desired temperature. Measurements were performed using a displacement of  $5 \times 10^{-4}$  rad and at a frequency of 0.1 Hz.

### 3. Results and discussion

#### 3.1. Verification of the calibration of the sensor signal in LTA

For each LTA measurement, the probe is placed onto the surface with a selected force (using force feedback). During the heating of the probe, the force feedback loop is open. Changes in the probe deflection, caused by, e.g. an expansion of the sample or a penetration of the tip into the sample, result in a change of the point of incidence of the laser beam on the four-quadrant photodetector. The recorded signal is transformed into the vertical displacement of the tip, which is the sensor signal recorded during LTA. Because the objective of this work is to characterise the skin layer thickness of BOPP films using a  $\mu$ TA operated in LTA-mode, first the calibration of the sensor signal is verified.

Thin films of PMMA spin-coated onto silicon wafers were selected as calibration materials. Fig. 1 shows typical results of LTA measurements for a film with a thickness of about 0.4  $\mu$ m, as estimated using spectroscopic ellipsometry. The sensor signal ( $S$ ) and its temperature-derivative

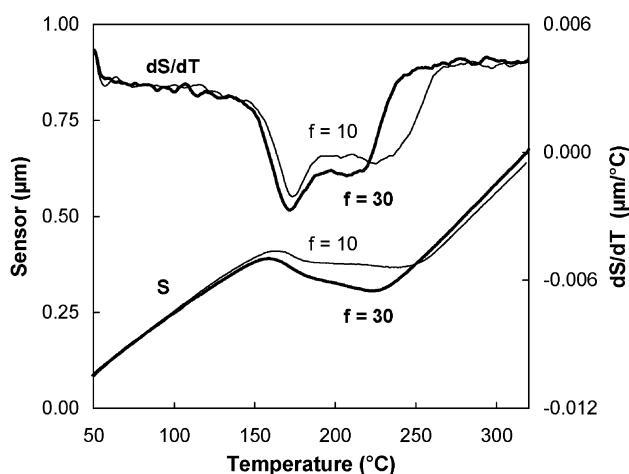


Fig. 1. LTA measurements on a PMMA-film spin-coated onto a silicon substrate: sensor ( $S$ ) and temperature-derivative of sensor ( $dS/dT$ ) versus temperature. Measured at 5 °C/s with contact forces corresponding to 10 nA (thin) and 30 nA (thick). Dashed lines illustrate calculation of skin layer thickness. Signals are average of 8 LTA measurements.

( $dS/dT$ ) are given. Initially, a gradual increase in the sensor signal due to thermal expansion is observed. Close to 140 °C, the probe tip penetrates into the PMMA. After a gradual penetration, a further increase in the sensor signal due to the thermal expansion of the substrate is seen.

The thickness of the film is  $0.44 \pm 0.01$   $\mu$ m (calculated as the step height at half height between the extrapolated tangents). However, one cannot be certain that this corresponds to the thickness of the PMMA layer, as some PMMA might remain between the probe tip and the silicon wafer. To verify this, the contact force was changed from 10 to 30 nA. At 30 nA, the penetration starts at the same temperature, but evolves faster: the thickness equals  $0.43 \pm 0.03$   $\mu$ m. Thus, the thickness obtained in the LTA analysis seems to correspond to the full film thickness.

To ascertain the accuracy of the measurement, a  $\mu$ TA procedure was developed to create a sample that enables one to measure the thickness of the film by surface imaging with the AFM in force feedback. In three thermolithographic steps, the PMMA layer is pyrolysed in a co-centred square with decreasing size. Details are given in Table 1.

Before and after each thermolithographic step, an image of the full range (100  $\mu$ m) was recorded (Fig. 2). The evolution of the topographic profile along a horizontal line in these images is given in Fig. 3. In the first thermolithographic step, a layer of 0.41  $\mu$ m is removed. A residual layer of about 25 nm thick is removed in the second lithographic step. After the third thermolithographic step, no further removal of material was detected: Thus, in the first two steps, the PMMA layer is (locally) removed; whereas the third step is needed to ensure that the removal is complete. The total thickness as evaluated from the difference between curves (a) and (c) around the centre of the square amounts to 0.44  $\mu$ m, in good agreement with the LTA results. This indicates that the thickness of a polymer film on a solid substrate can be determined using through-thickness LTA measurements.

It is important to note that the evolution of the penetration observed in  $\mu$ TA is determined by the evolution of the melt viscosity, rather than just by the glass transition. For the film of PMMA with a molar mass of 93,300 g mol<sup>-1</sup>, the penetration of the probe in the PMMA layer sets in around 120 °C (first

Table 1  
 $\mu$ TA procedure for creating a reference sample by thermolithography

Step	Purpose	T-probe (°C)	Range ( $\mu$ m)	Rate ( $\mu$ m/s)
1	Image surface (a)	50	100	100
2	Pyrolyse polymer layer	550	30	100
3	Image surface (b)	50	100	100
4	Pyrolyse polymer layer	550	20	20
5	Image surface (c)	50	100	100
6	Pyrolyse polymer layer	550	10	10
7	Image surface (d)	50	100	100

In all steps, the Wollaston probe was scanned over the surface in a co-centred square at a resolution of 200 lines.

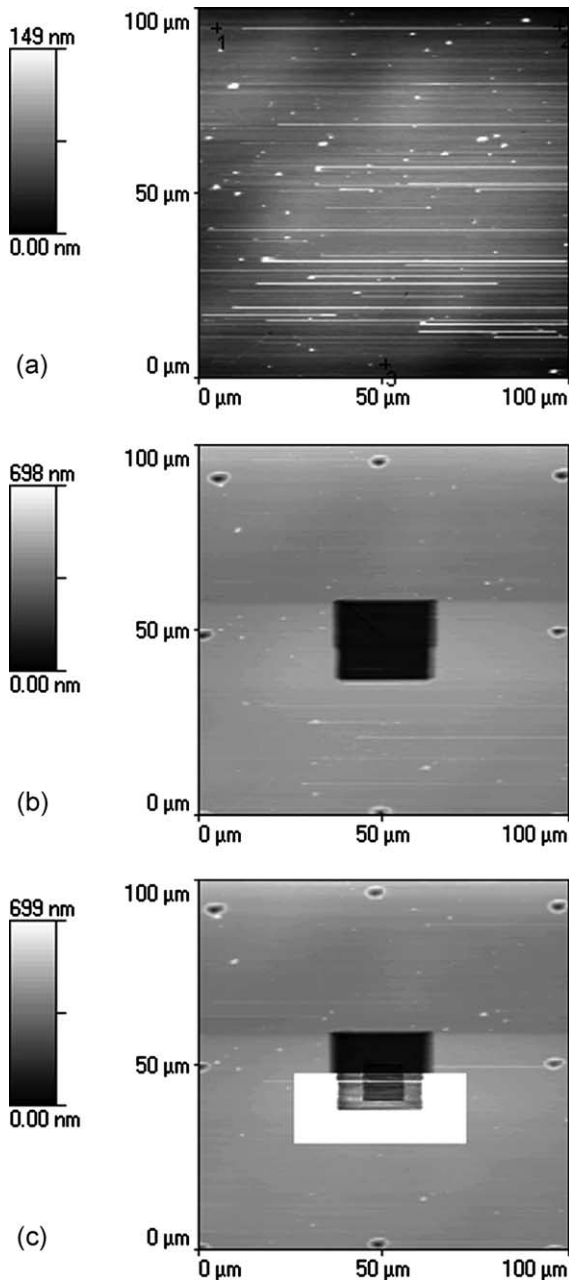


Fig. 2. Topography images taken at different stages of the thermolithography procedure for a PMMA film on a silicon substrate ((a), (b), (c) see Table 1) showing the same  $100 \times 100 \mu\text{m}^2$  area. Inset in image (c) zoom to a 0–100 nm height range for the bottom of the pyrolysed area.

deviation from baseline in  $dS/dT$ ) and is mainly occurring near  $150^\circ\text{C}$  (Fig. 1). The latter is well above the glass transition of this PMMA as determined by MTDSC ( $114^\circ\text{C}$ ). To confirm the influence of the melt viscosity on the penetration of the probe, bulk PMMA samples with molar masses of 15,000–350,000  $\text{g mol}^{-1}$  were studied. Although the glass transition temperatures of these materials differ  $6^\circ\text{C}$  only, the penetration of the probe is markedly influenced (Fig. 4). With increasing molar mass, the melt viscosity increases strongly, resulting in a slower penetration.

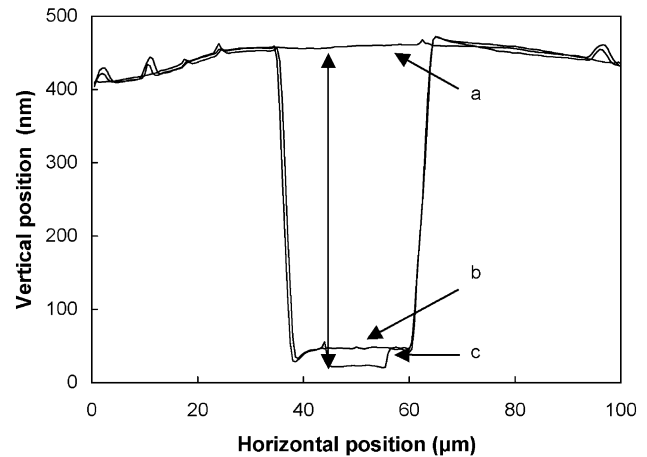


Fig. 3. Topography profile at different stages of the thermolithographic procedure for a PMMA film on a silicon substrate. Curves correspond to average height along a 5-pixels wide horizontal band near centre of topography images ((a), (b), (c) see Fig. 2 and Table 1). Total thickness equals  $0.44 \mu\text{m}$  (indicated by vertical arrow).

### 3.2. Melting behaviour of raw materials of BOPP films

Before discussing the BOPP films, first the analysis of the constituting core and skin layer materials will be focussed on. First, the melting behaviour of the bulk skin and core layer materials were studied using DSC. The thermograms of a heating at  $10^\circ\text{C}/\text{min}$  after a controlled cooling at  $10^\circ\text{C}/\text{min}$  from a temperature about  $20^\circ\text{C}$  above the end of the melting range are given in Fig. 5. For the core layer material (iPP), a sharp melting endotherm is observed, with a maximum at  $163.0^\circ\text{C}$  and an endset at  $168.9^\circ\text{C}$ . The melting range of the skin layer material is much broader, with an important fraction between room temperature and  $75^\circ\text{C}$ , a range where hardly any melting is observed for iPP. The melting endotherm of the skin layer material has a maximum at  $128.4^\circ\text{C}$  and an end-set near  $148.5^\circ\text{C}$ . At the

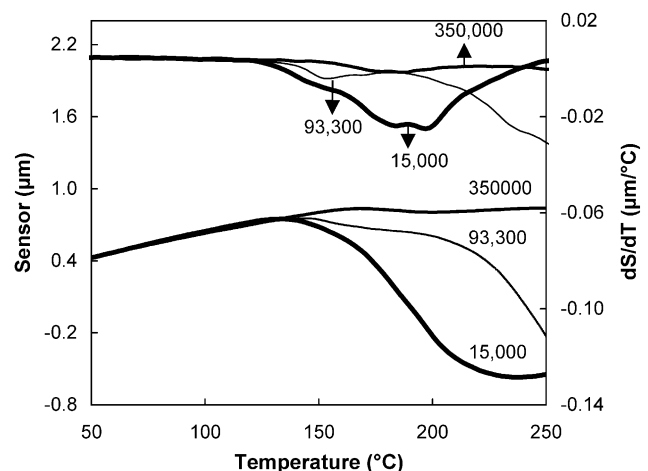


Fig. 4. LTA measurements on bulk PMMA sample: sensor ( $S$ ) and temperature-derivative of sensor ( $dS/dT$ ) versus temperature for PMMA of a molar mass of 15,000  $\text{g mol}^{-1}$  ( $T_g = 109^\circ\text{C}$ ); 93,300  $\text{g mol}^{-1}$  ( $T_g = 114^\circ\text{C}$ ), and 350,000  $\text{g mol}^{-1}$  ( $T_g = 115^\circ\text{C}$ ).

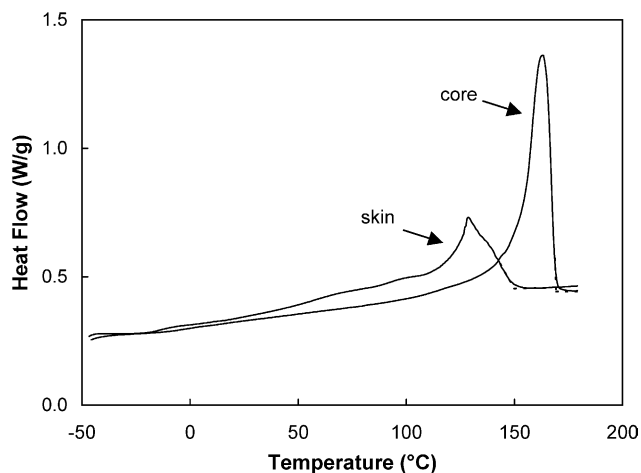


Fig. 5. Melting of bulk skin and core layer materials studied by DSC. Heating at 10 °C/min after cooling at 10 °C/min from 20 °C above the melting range.

latter temperature, the major part of the iPP melting still has to occur. It is the lower melting range of the skin layer material (copolymer) compared to the core layer material (iPP) that enables one to determine the thickness of the skin layer by the through-thickness micro-thermal analysis approach discussed in the next paragraph.

The  $\mu$ TA results for the bulk samples of skin and core layer materials are depicted in Fig. 6. For the melting of the skin layer material, the onset of the peak in  $dS/dT$  equals 128.5 °C, which corresponds to the maximum of the melting range measured in DSC. The slowing of the penetration observed for the skin layer material is due to the reduction of the force exercised by the probe tip on the material as the deflection of the cantilever gradually relaxes (the tip penetrates into the material while the piezzo-electric element is kept in a fixed position). For the iPP core layer material, no clear correspondence between  $\mu$ TA and DSC is observed: the onset of the peak in  $dS/dT$  is at 197 °C, or

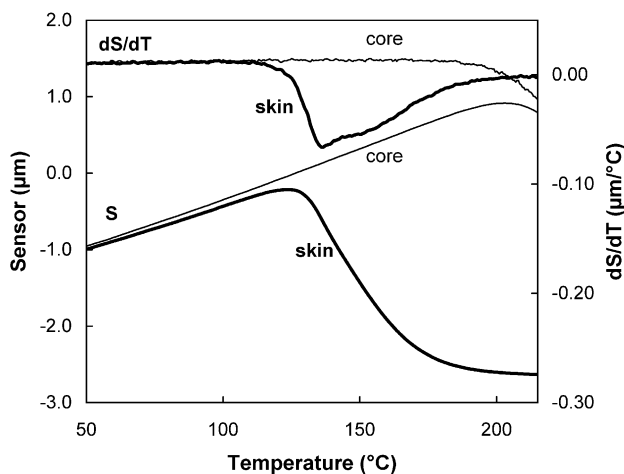


Fig. 6. LTA measurements on bulk skin layer and core layer materials: sensor signal ( $S$ ) and its temperature-derivative ( $dS/dT$ ) for heating at 15 °C/s.

more than 25 °C above the peak melting temperature observed in DSC. The delayed penetration of the probe into the core layer material might originate from a higher melt viscosity. Dynamic rheometry measurements performed on the raw materials confirm that the melt viscosity of the iPP is more than twice the one of the skin layer material (both evaluated at a temperature of 20 °C above the end of the melting range).

In addition to effects of the melt viscosity, the following factors should be taken into account for a quantitative comparison of the results: (1) the penetration of the probe into the material can be expected to occur once most of the crystals are molten, so close to the end of the melting range, (2) superheating of the polymer crystals might occur at the higher heating rate (5 K s<sup>-1</sup>) used in LTA, (3), the temperature accuracy of the LTA measurements is estimated to be 5 °C.

Since the temperature difference between the onset of the penetration in the skin and the core layer measured by  $\mu$ TA (ca. 50 °C, Fig. 6) is much larger than the difference in the peak maximum (ca. 35 °C) or the endset (ca. 20 °C) of the melting endotherms observed in DSC (Fig. 5), the possibility of resolving the two transitions in a through-thickness  $\mu$ TA measurement is even higher than expected from DSC results.

### 3.3. Micro-thermal analyses on layered BOPP films

Fig. 7 shows a typical result of an LTA measurement on a BOPP-film. In this case, the power signal,  $P$ , a measure of the amount of power transferred from the probe to the sample, is given as well.

In the sensor signal, two step-wise decreases are observed, with their corresponding peaks in the temperature-derivative. These step-wise decreases are due to the penetration of the probe into the skin and core layers, consecutively. The first step sets in near 130 °C, which is close to the peak melting temperature (DSC, Fig. 5) and the

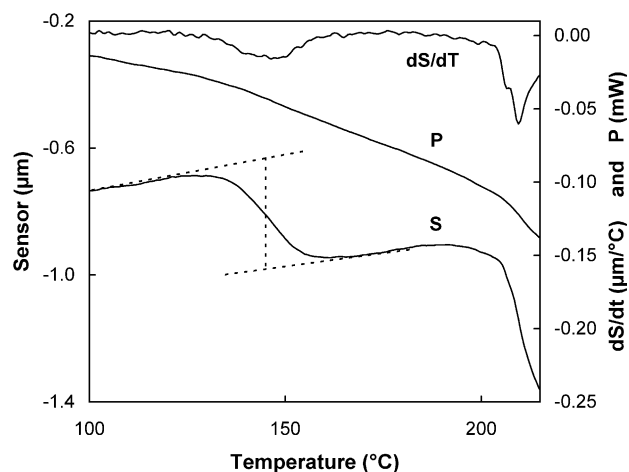


Fig. 7. LTA measurement on a BOPP film: sensor ( $S$ ), temperature-derivative of sensor ( $dS/dT$ ), and power ( $P$ ) signal versus temperature for a heating at 5 °C/s. Dashed lines illustrate calculation of skin layer thickness.

onset of  $dS/dT$  ( $\mu$ TA, Fig. 6) observed for the bulk skin layer material. After a penetration of about  $0.4 \mu\text{m}$ , the sensor signal levels off. It even increases again because the rate of penetration becomes less than the increase due to thermal expansion. Subsequently, the core layer melts: the penetration of the probe into the material accelerates again around  $180 \text{ }^\circ\text{C}$ . This is more than  $25 \text{ }^\circ\text{C}$  above the DSC peak melting temperature for the bulk iPP core layer material, as was the case for the  $\mu$ TA measurement on the bulk material.

In the power signal, again two steps can be distinguished. As the material melts, the probe penetrates into it. Thus, the contact area between the probe tip and the melting material increases, increasing the amount of power needed to maintain the probe tip at a certain temperature. As, the active tip of the probe is a  $5 \mu\text{m}$  wire (bent with a  $25 \mu\text{m}$  radius), a penetration of a few tenths of a micrometer will strongly increase the contact area. As a result, the power and sensor signals are convoluted.

The repeatability of the LTA measurements is very good, as shown for the sensor signal in Fig. 8. This points to the lateral structural homogeneity of the film. In topographic images recorded with the Wollaston probe, the smoothness of the films is obvious from the  $250 \text{ nm}$  peak-to-peak height variation over an area of  $100 \times 100 \mu\text{m}^2$  (Fig. 9). Since the skin layer material is laterally homogeneous, no contrast was detected in the conductivity images.

The step height of the penetration through the skin layer can be used as a measure of the layer thickness (Fig. 7 for calculation method). For most samples, the thickness was determined by averaging the results of 15 LTA measurements distributed by five over three  $100 \times 100 \mu\text{m}^2$  areas. The standard deviation on the 15 values is given as error margin. For the film in Fig. 6, the  $\mu$ TA thickness of  $0.33 \pm 0.03 \mu\text{m}$  compares well with the skin layer thickness of  $0.34 \pm 0.10 \mu\text{m}$  measured by TEM. Representative TEM images are shown in Fig. 10.

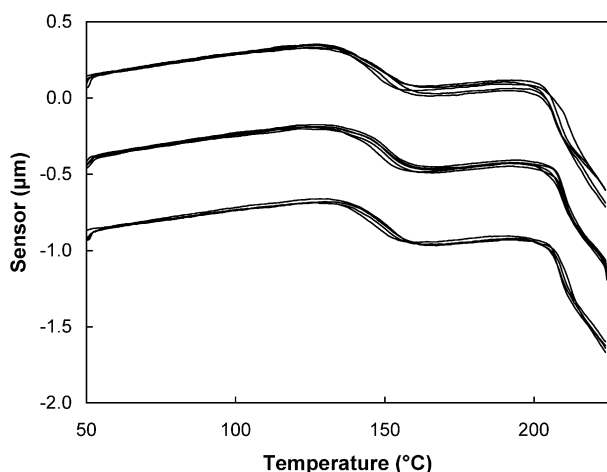


Fig. 8. Repeatability of sensor signal for LTA measurements on a BOPP film for a heating at  $5 \text{ }^\circ\text{C/s}$ . Fifteen LTA measurements consisting of three series of five measurements in locations evenly distributed over three  $100 \times 100 \mu\text{m}^2$  areas on a single  $4 \times 4 \text{ mm}^2$  sample. Series were vertically shifted by  $0.5 \mu\text{m}$ .

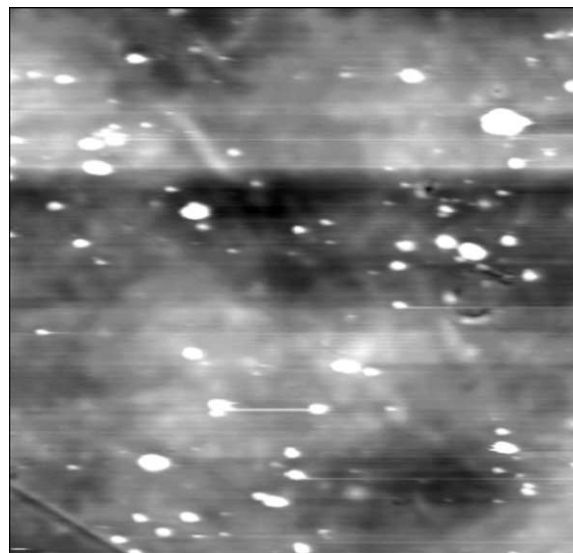


Fig. 9. Topography image of a BOPP film showing a  $100 \times 100 \mu\text{m}^2$  area. Height scale  $0\text{--}210 \text{ nm}$ .

#### 3.4. Influence of experimental conditions for LTA

The experimental parameters that are most likely to affect the thickness measurement are the contact force applied at the start of the LTA measurement and the heating rate or temperature program used.

For a film of about  $0.8 \mu\text{m}$  thickness, a series of three times three LTA's was performed on a single  $100 \times 100 \mu\text{m}^2$  with forces corresponding to 10, 30, and 50 nA and using a  $5 \text{ }^\circ\text{C/s}$  heating rate. The average of the three measurements is shown in Fig. 11. The thickness is evaluated at  $0.76$  and  $0.78 \mu\text{m}$  for 10 and 50 nA, respectively. At higher forces, an earlier and more gradual onset of the penetration into the skin layer is observed. Comparison with the DSC results indicates that at higher forces the probe penetrates into the skin layer while it is still partially crystalline. Because the gradual onset of the penetration at higher contact forces complicates the selection of the tangent for thickness evaluation, the use of a force corresponding to 10 nA was preferred.

The effect of the heating rate on the penetration of the probe is shown in Fig. 12. The evaluated thickness is not significantly different and the resolution of the two transitions is not markedly influenced. Therefore, the  $5 \text{ }^\circ\text{C/s}$  heating rate was chosen.

#### 3.5. Comparison $\mu$ TA and TEM analysis of layer thickness

For films with a skin layer thickness ranging from about  $0.1$  to  $1.6 \mu\text{m}$  (as determined from TEM images), the skin layer thickness was measured by through-thickness  $\mu$ TA experiments. The results are compared in Fig. 13. For the range studied, a linear regression on the data results in a slope of  $0.98 \pm 0.04 \mu\text{m}/\mu\text{m}$ , a  $0.00 \pm 0.02 \mu\text{m}$  intercept and a

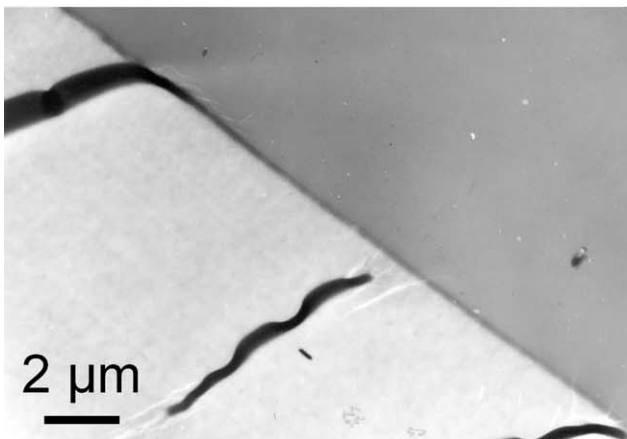
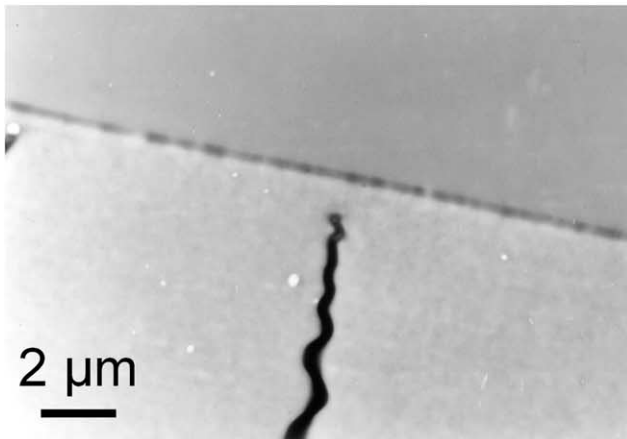
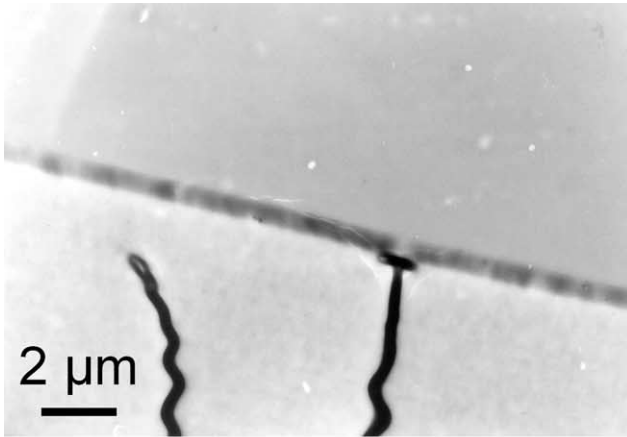


Fig. 10. TEM images of cross sections of BOPP films used for estimating the thickness of the skin layer. Estimated thickness: (a) 0.6  $\mu\text{m}$ ; (b) 0.2  $\mu\text{m}$ ; (c) 0.1  $\mu\text{m}$ .

correlation coefficient  $r^2$  of 0.96. Thus, a one-to-one correspondence between the results of  $\mu\text{TA}$  and TEM is found.

#### 4. Conclusions

Although the DSC melting temperatures of the skin layer and the core layer are only about 15  $^{\circ}\text{C}$  different, it proved to

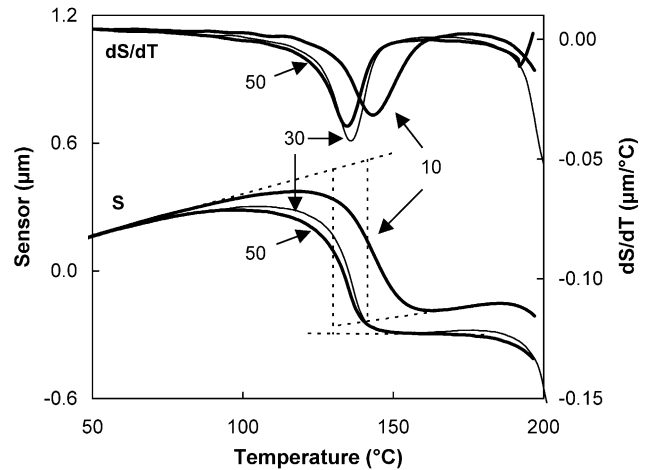


Fig. 11. Influence of contact force on LTA measurement for a BOPP film with a skin layer of 0.7  $\mu\text{m}$  (TEM): sensor signal ( $S$ ) and its temperature-derivative ( $dS/dT$ ) for a heating at 5  $^{\circ}\text{C}/\text{s}$  with contact forces corresponding to 10, 30, and 50 nA. Each curve is the average of the result for three LTA locations. All nine locations are within one  $100 \times 100 \mu\text{m}^2$  area.

be possible to determine in situ the thickness of the skin layer by through-thickness local thermal analysis with a  $\mu\text{TA}$ . These measurements are made directly on the film, avoiding the complications of sample embedding and microtomy involved in TEM analysis. The film thickness obtained for standard  $\mu\text{TA}$  conditions correlates well with the thickness observed by TEM. Variations in the contact force and heating rate did not strongly influence the  $\mu\text{TA}$  results. Thus, the through-thickness local thermal analysis procedure is robust, accurate, and, last but not least, fast. It allows for a relatively quick analysis and therefore complements TEM for analysing BOPP films.

The presented approach of through-thickness local thermal analysis can be used for other layered structures.

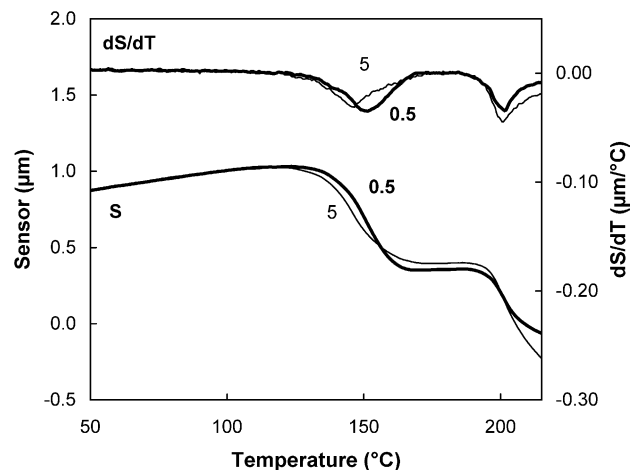


Fig. 12. Influence of heating rate on LTA measurement for a BOPP film with a skin layer of 0.7  $\mu\text{m}$  (TEM): sensor signal ( $S$ ) and its temperature-derivative ( $dS/dT$ ) for a heating at 0.5 and 5  $^{\circ}\text{C}/\text{s}$  with a contact force corresponding to 10 nA. Each curve is the average of the results for three LTA locations.

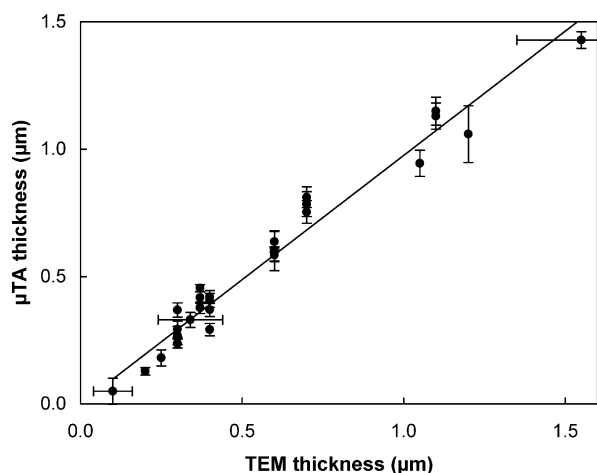


Fig. 13. Skin layer thickness determined by through-thickness LTA using a  $\mu$ TA versus thickness determined by TEM. Solid line: result of linear regression. Vertical and horizontal bars indicate standard deviation on  $\mu$ TA and TEM measurements, respectively.

It could, e.g. also be used to determine the thickness of a coating on fibres or generally of (thin) polymer films on solid substrates. Of course, the technique is limited to samples with a sufficiently low thickness of the outer layer to allow for the probe to penetrate completely through the layer. This limits the range to a few micrometers. Moreover,

the thermal transitions and the chemorheological behaviour of the skin and core layer or substrate materials, in particular their melting temperature difference and melt viscosities, are expected to determine the measurement feasibility.

### Acknowledgements

Guy Van Assche is a postdoctoral researcher of the Fund for Scientific Research FWO-Flanders (Belgium). This work was supported by research grants from the Fund for Scientific Research FWO-Flanders (Belgium) and the Research Council of the Vrije Universiteit Brussel (VUB). Spectroscopic ellipsometry measurements were performed by Jan De Laet (VUB) at IMEC (Belgium).

### References

- [1] Agrawal GD, Mannan SM. *Chem Eng World* 1995;30(5):33–6.
- [2] Price DM, Reading M, Hammiche A, Pollock HM. *Int J Pharmacol* 1999;192(1):85–96.
- [3] Pollock HM, Hammiche A. *J Phys D Appl Phys* 2001;34(9):R23–R53.
- [4] Abad MJ, Ares A, Barral L, Cano J, Diez FJ, Lopez J, et al. *J Appl Polym Sci* 2002;85(7):1553–61.